Quantification of microtubule nucleation, growth and dynamics in wound-edge cells

Kimberly J. Salaycik, Carey J. Fagerstrom, Kausalya Murthy, U. Serdar Tulu and Patricia Wadsworth*

Department of Biology, Program in Molecular and Cellular Biology, University of Massachusetts, Amherst, MA 01003, USA

*Author for correspondence (e-mail: patw@bio.umass.edu)

Accepted 7 June 2005
Journal of Cell Science 118, 4113-4122 Published by The Company of Biologists 2005
doi:10.1242/jcs.02531

Summary

Mammalian cells develop a polarized morphology and migrate directionally into a wound in a monolayer culture. To understand how microtubules contribute to these processes, we used GFP-tubulin to measure dynamic instability and GFP-EB1, a protein that marks microtubule plus-ends, to measure microtubule growth events at the centrosome and cell periphery. Growth events at the centrosome, or nucleation, do not show directional bias, but are equivalent toward and away from the wound. Cells with two centrosomes nucleated approximately twice as many microtubules/minute as cells with one centrosome. The average number of growing microtubules per μm^2 at the cell periphery is similar for leading and trailing edges and for cells containing one or two centrosomes. In contrast to microtubule growth, measurement of the parameters of microtubule dynamic instability demonstrate that microtubules in the trailing edge are more dynamic than those in the leading edge. Inhibition of Rho with C3 transferase had no detectable effect on microtubule dynamics in the leading edge, but stimulated microtubule turnover in the trailing edge. Our data demonstrate that in wound-edge cells, microtubule nucleation is non-polarized, in contrast to microtubule dynamic instability, which is highly polarized, and that factors in addition to Rho contribute to microtubule stabilization.

Supplementary material available online at
http://jcs.biologists.org/cgi/content/full/118/18/4113/DC1

Key words: GFP-EB1, centrosome, polarity, Rho

Introduction

Microtubules are cytoskeletal polymers that are required for intracellular transport of vesicular cargo, for control of cell shape, for spindle assembly and for chromosome motion during mitosis. Although microtubules contribute to cell structure and organization, they are highly dynamic polymers. In vitro and in vivo microtubules display a non-equilibrium behavior called dynamic instability in which microtubules lengthen and shorten by the addition and loss of subunits from the polymer ends (Mitchison and Kirschner, 1984). Dynamic instability behavior is cell-type-specific (Cassimeris, 1993; Sammak and Borisy, 1988; Schulze and Kirschner, 1988; Shelden and Wadsworth, 1993). However, early studies of microtubule behavior in living cells were limited to the cell periphery, where individual microtubule ends could be detected and their behavior quantified. More recently, it has become clear that a complete understanding of microtubule behavior requires knowledge of events in the central cytoplasm and at the centrosome. Using cytoplasts, which contain a reduced microtubule array, and pattern photobleaching of intact cells, Komorova and colleagues have demonstrated that microtubules in the cell interior show highly persistent growth, not dynamic instability (Komarova et al., 2002). When these persistently growing microtubules reach the cell margin they switch to dynamic instability behavior (Komarova et al., 2002). Microtubule behavior at the centrosome has also been difficult to examine, given the high density of microtubules in this region. Recently, GFP-tagged EB1, a protein that marks growing microtubule ends, has been used to quantify microtubule nucleation throughout the cell cycle (Piehl et al., 2004). With these improved methods, microtubule behavior including 'birth' at the centrosome and events in the interior cytoplasm and periphery can be quantified in living cells and their contribution to microtubule organization and cell behavior determined.

Microtubules are required for the establishment and maintenance of a polarized cellular morphology (Vasiliev, 1991). Early studies identified a subset of post-translationally modified microtubules that are oriented toward the direction of cell migration and are resistant to depolymerization by nocodazole (Gundersen and Bulinski, 1988). Although post-translational modification is a consequence, not a cause of stability (Khawaja et al., 1988), the distribution of these microtubules led to the idea that stabilized microtubules contribute to cell polarity and directed migration. Subsequent studies on various types of motile cells, however, show that dynamic microtubules are required for cell migration. For example, inhibition of microtubule dynamics with low doses of microtubule poisons reduces cell migration into a wound in monolayer cultures (Liao et al., 1995). Examination of microtubule dynamics in living newt lung epithelial cells shows that microtubules in the extending lamellae at the leading edge are dynamic, whereas microtubules in lamellae that contact neighboring cells can be dynamic or stabilized (Waterman-Storer et al., 2000). Dynamic 'pioneer' microtubules have also been observed in extending nerve

growth cones and lamella of various cells (Suter and Forscher, 1998; Tanaka and Kirschner, 1991; Wadsworth, 1999; Waterman-Storer and Salmon, 1997). In growth cones, local stabilization of microtubules induces growth cone turning, indicating that both dynamic and stable populations of microtubules may contribute to directed cell migration (Buck and Zheng, 2002).

The selective stabilization model, proposed nearly twenty years ago, hypothesizes that microtubules grow uniformly from a microtubule organizing center (MTOC) and are subsequently stabilized (Alberts et al., 2002; Kirschner and Mitchinson, 1986). In the experiments reported here, we examine the selective stabilization model in fibroblasts and epithelial cells by measuring microtubule behavior at the centrosome and in the leading and trailing edges of wound-edge cells (Yvon et al., 2002). Using EB1-GFP to mark microtubule plus-ends, we demonstrate that microtubule nucleation from the centrosome is not biased with respect to overall cell polarity and microtubule growth events/unit area in the periphery are similar in leading and trailing edges. The number of microtubule growth events/area is also constant throughout the cell cycle, even as centrosome duplication results in nearly twice as many nucleation events. Unlike microtubule growth, however, microtubule catastrophe, pause and overall dynamicity are highly spatially regulated, with microtubules in trailing edges showing more dynamic behavior than microtubules in leading edges. Surprisingly, inhibition of RhoA did not have an effect on microtubule behavior in leading edges, but did enhance microtubule turnover in trailing edges. In summary, our data demonstrate that polarized cells generate non-polarized arrays of growing microtubules and that this distribution of growing microtubule plus-ends is maintained even as microtubules become locally stabilized.

Materials and Methods

Materials

All materials for cell culture were obtained from Sigma (St Louis, MO, USA), with the exception of fetal calf serum, which was obtained from Atlanta Biologicals (Norcross, GA, USA) and OptiMEM and trypsin, which were obtained from Invitrogen (Carlsbad, CA, USA). Unless otherwise noted, all other chemicals were obtained from Sigma Chemical (St Louis, MO, USA).

Cell culture and transfection

Porcine kidney epithelial cells, LLCPK1 (American Type Culture Collection, Manassas, VA, USA) and LLCPK1 cells permanently expressing EB1-GFP (Piehl and Cassimeris, 2003), or GFP-α-tubulin (Rusan et al., 2001) were grown at 37°C and 5% CO_2 in a 1:1 mix of Ham's F10 and OptiMEM supplemented with 7.5% fetal calf serum and antibiotic/antimycotic. Chinese hamster ovary (CHO) cells (Kao and Puck, 1968; Rodionov et al., 1999) were cultured under the same conditions in Ham's F-10 with 10% fetal calf serum. For observation, cells were plated on 23 mm, grid-etched coverslips (Bellco Glass, Vineland, NJ, USA) and allowed to grow to confluence before wounding. Monolayers were manually wounded with forceps, incubated for 4 hours, and subsequently used for immunocytochemistry or for microinjection. Coverslips with cells for live cell imaging were placed in Rose chambers (Rose et al., 1958) containing DMEM that was bicarbonate free and contained Hepes buffer, 20 mM, pH 7.25. This DMEM also lacked indicator dye and contained 0.3 U/ml Oxyrase oxygen scavenging system (EC Oxyrase, Mansfield, OH, USA) to reduce photobleaching.

For transient transfection with EB1-GFP (Piehl and Cassimeris, 2003), or GFP-tubulin (Rusan et al., 2001) we used Lipofectamine2000 (Invitrogen, Carlsbad, CA, USA) according to the manufacturer's directions. Cells were allowed to recover for 2 days before experimental analysis. For CHO cells transfected with EB1-GFP, only cells with EB1-GFP restricted to the plus-ends of microtubules, and with an overall level of expression comparable to the LLCPK1-EB1-GFP cell line were used for analysis. For GFP-tubulin-transfected cells, only cells with a moderate level of expression in which individual microtubules could be detected, and with no aberrant microtubule bundles, were analyzed.

Indirect immunofluorescence staining

For tubulin staining, cells were rinsed twice in Ca^{2+}- and Mg^{2+}-free PBS, then rinsed for 8 seconds in Karsenti's extraction buffer (consisting of 80 mM Pipes, 5 mM EGTA, 1 mM $MgSO_4$ and 0.5% Triton X-100) fixed in –20°C methanol for 10 minutes, rehydrated in Ca^{2+}- and Mg^{2+}-free PBS containing 0.1% Tween 20 and 0.02% sodium azide (PBS-Tw-Azide). Cells were incubated in equal parts of primary antibody to α-tubulin (YL1/2, Accurate Chemical, Westbury, NY, USA) and 2% BSA for 1 hour at 37°C, rinsed in PBS-Tw-Azide and incubated with fluorescein-conjugated goat anti-rat (Sigma, St Louis, MO, USA; 1:32 dilution) secondary antibodies. To stain for both tubulin and myc, cells were rinsed in Ca^{2+}- and Mg^{2+}-free PBS, fixed in 0.25% glutaraldehyde for 1 minute followed by 1 minute in Karsenti's extraction buffer, an additional 5 minutes in glutaraldehyde fix, and 10 minutes in 1% sodium borohydride in PBS-Tw-Azide. The primary and secondary antibodies for tubulin were as just described; the primary antibody for myc was clone 9E10, from Sigma, followed by rhodamine-conjugated anti-mouse secondary antibodies, also from Sigma. Cells were mounted in Vectashield (Vector Laboratories, Burlingame, CA, USA) and sealed with clear nail polish.

Microinjection

Cells were microinjected into the nucleus with constructs expressing myc-tagged Cdc42-L61 and Rho-N19 (generous gifts from Allan Hall) as described previously (Ridley and Hall, 1992) at a needle concentration of 250-750 μg/ml. Cells in a confluent monolayer were injected 1 hour post-wounding and incubated for an additional 3 hours to allow expression of the injected construct. Injected cells were fixed and stained for α-tubulin and for myc. C3 transferase was used as described previously (Yvon and Wadsworth, 1997) at a concentration of 50-100 μg/ml.

Image acquisition and data analysis

Live cells expressing GFP α-tubulin or EB1-GFP were observed with a Nikon Eclipse TE 300 inverted microscope equipped with a 100× 1.3 numerical aperture objective lens and coupled to a Perkin-Elmer spinning disc confocal scan head (Perkin Elmer). Images were acquired with a Princeton Instruments Micromax interline transfer cooled CCD camera (Roper Instruments, NJ, USA) and MetaMorph Software (Universal Imaging, Brandywine, PA, USA). Time-lapse sequences of GFP and phase images were initiated 4 hours after wounding and were collected with an exposure time of 0.3-0.7 seconds at an interval of 2 seconds for a total time of approximately 3 minutes.

Fixed cells stained for microtubules were imaged as just described for live cells. In some cases, a complete Z-stack of images was collected using a p-721 piezo nano-focusing device (Physik Instruments, Auburn, MA) (Rusan and Wadsworth, 2005). Fixed cells stained for both microtubules and myc were imaged using a Zeiss 510

Meta confocal microscope as previously described (Murthy and Wadsworth, 2005).

Microtubule density data was obtained for leading and trailing regions by outlining the region of interest using Metamorph and measuring the average fluorescence intensity per pixel. The background intensity, determined by selecting an area lacking microtubules, was subtracted from these values. For these measurements, we used a single Z-plane rather than a Z-stack. These cells are very flat and the plane of focus (~1 μm in Z dimension) was selected so as to include the majority of microtubules in the lamellar region.

Measurement of microtubule nucleation and growth using EB1-GFP

To determine nucleation events using EB1- GFP, we counted EB1-GFP dashes emerging from the centrosome over time. For calculating directional EB1-GFP growth events at the centrosome, the line tool function of Metamorph imaging software was used to separate the cell into leading and trailing halves. The number of EB1-GFP growth events that originated from the centrosome and traveled toward each half was quantified for the entire duration of time-lapse movies and expressed as nucleations/unit time. To measure microtubule growth events in the periphery of wound-edge cells, the peripheral region was divided into subregions to facilitate accurate counting of the EB1-GFP comets. The subregions were boxes of known dimensions, generated using the region of interest function in MetaMorph, and were aligned around the periphery of each cell. The number of EB1-GFP growth events was quantified for the entire duration of time-lapse movies in each subregion. From the known dimensions of each subregion, the average number of EB1-GFP spots/unit area was then determined. Area was measured in square microns.

Microtubule growth rate and dynamic instability

Microtubule growth rates were obtained by tracking EB1-GFP comets at microtubule plus-ends using the 'track points' function of Metamorph, linked to an Excel spreadsheet. Instantaneous rates were determined using successive points. Microtubule tracking was performed using Metamorph Imaging Software as previously described in detail (Rusan et al., 2001); statistical analysis was performed using MINITAB for windows (release 12). Note that microtubule growth rates determined using EB1-GFP are faster than those measured using GFP-tubulin. The reason for this discrepancy is that in the case of EB1-GFP instantaneous rates were determined, and EB1-GFP only labels microtubules that are growing. In the GFP-tubulin cells, the rate of growth is determined from the slope of growth phases in a distance versus time plot. Slight pauses of the microtubule may be included in the measurement, thus reducing the apparent growth rate.

Results

Microtubule distribution in wound-edge cells

In previous work, we demonstrated that centrosome reorientation occurs in CHO fibroblasts, but not epithelial cells (Yvon et al., 2002). In contrast to the cell-type-specific behavior of the centrosome, we observed that both types of wound-edge cells are characterized by an asymmetric microtubule array with more microtubules extending toward the wound edge than away (Fig. 1A-D). Microtubule fluorescence intensity measurements reveal a statistically significant increase in microtubule density in leading, as compared with, trailing edges of both cell lines. In living cells, the ratio of leading to trailing intensity was 2.8±1.1 for CHO and in 1.7±0.4 for LLCPK1 (Fig. 1C,D). Because previous work has shown that the small GTPase, Cdc42, is required for the generation and maintenance of cell polarity (Hall, 1998), we examined microtubule distribution in cells expressing a constitutively active form of Cdc42 (L61Cdc42). Consistent with previous work, expression of L61Cdc42 results in a loss of cell polarity, with lamellar protrusions extending all around the cell periphery and a loss of the asymmetry in microtubule organization (ratio of leading to trailing intensity of 1.29±0.3) (Fig. 1E). The small GTPase Rho is required for stress fiber formation (Hall, 1998) and the generation of post-translationally modified Glu microtubules (Cook et al., 1998). In cells expressing a dominant-negative RhoA construct (N19RhoA), an asymmetric microtubule array that was indistinguishable from controls was observed (ratio of leading to trailing intensity of 2.1±0.2) (Fig. 1F). Thus, misregulation of Cdc42, but not RhoA, interferes with the generation of an asymmetric microtubule array in wound-edge cells.

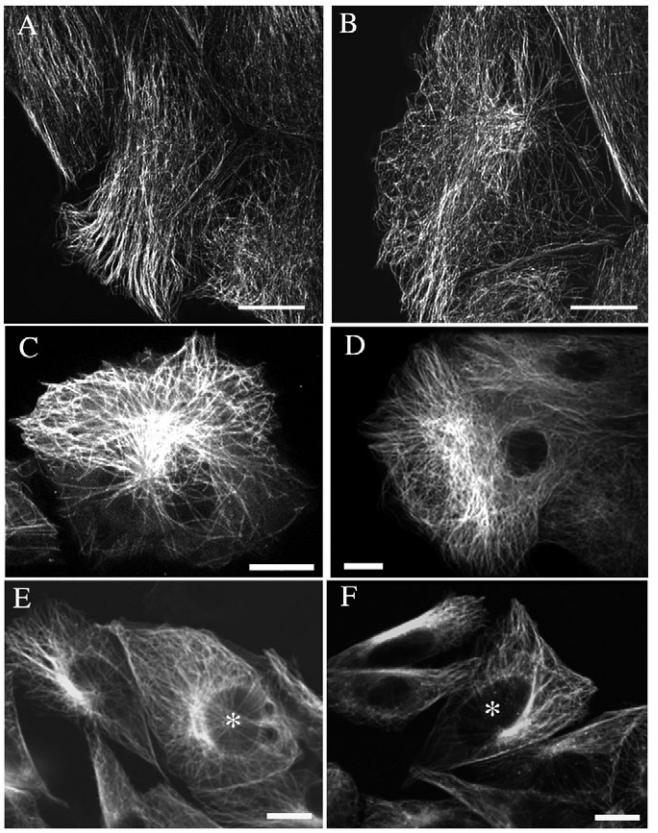

Fig. 1. Microtubule organization is asymmetric in wound-edge cells. (A,B) Maximum intensity projections showing the distribution of microtubules in wound-edge LLCPK1 (A) and CHO (B) cells fixed and stained with antibodies to tubulin. (C) CHO and (D) LLCPK1 cells expressing GFP-tubulin shows the asymmetric distribution of microtubules. (E,F) Microtubule distribution in wound-edge CHO cells expressing a constitutively active form of Cdc42 (L61Cdc42) (E, right cell, marked with asterisk) and uninjected control cells (E, left cell) and expressing dominant negative N19 RhoA (F, injected cell marked with asterisk). Microtubule distribution is asymmetric in control and N19 RhoA-expressing cells but not in L61 Cdc42-expressing cells. Scale bars: 10 μm.

Microtubule growth at the centrosome in wound-edge cells

To determine what features of microtubule behavior might contribute to polarized microtubule organization we measured microtubule growth events at the centrosome in cells expressing EB1-GFP to mark the plus-ends of growing microtubules. Recent work has demonstrated that EB1-GFP comets emerging from the centrosome co-localize with newly polymerized microtubules, indicating that EB1-GFP labeling represents an early step in microtubule growth that we will refer to as nucleation (Piehl and Cassimeris, 2003; Piehl et al., 2004). In many cells, dashes of EB1-GFP fluorescence originated from a single site and staining of these cells with antibodies to γ-tubulin demonstrate that this site corresponds to the centrosome (data not shown). These cells, which contain a single centrosome and single site from which EB1-GFP dashes emerge, are classified as G1. In other cells, EB1-GFP fluorescence was observed to originate from two sites, corresponding to the duplicated centrosomes; these cells are therefore in G2. The two centrosomes could be adjacent to each other, or spatially separated.

To examine microtubule nucleation from the centrosome we used an LLCPK1 cell line stably expressing EB1-GFP (Piehl and Cassimeris, 2003). Previous work demonstrated that expression of GFP-tagged EB1 did not interfere with microtubule growth or cell behavior (Piehl and Cassimeris, 2003). In these cells, the average number of growth events/minute at the centrosome in non-wound-edge G1 cells was 14.1±5.8; in non-wound-edge cells in G2 the rate of nucleation from the two centrosomes was 22.4±5.8. These values were not significantly different in LLCPK1-EB1-GFP cells at the wound edge (13.9±1.5 in G1 and 18.5±2.3 in G2) demonstrating that nucleation at the centrosome is not changed in epithelial cells when motility and polarization are induced by wounding the monolayer (Fig. 2E-H; see Movie 1 in supplementary material). To measure microtubule nucleation in CHO fibroblasts, we transiently tranfected cells with EB1-GFP and selected cells in which microtubules were labeled at the plus-ends, not along the microtubule length, and with a fluorescence intensity similar to the previously characterized LLCPK1-EB1-GFP cell line (see Materials and Methods). In these cells, the rate of nucleation was 14.4±1.7 in G1 cells and 23.1±3.7 in G2 cells, remarkably similar to the values obtained in epithelial cells, suggesting that rate of microtubule nucleation from the centrosome in control, non-wound-edge cells is not cell-type-specific (Table 1, Fig. 2A). In wound-edge

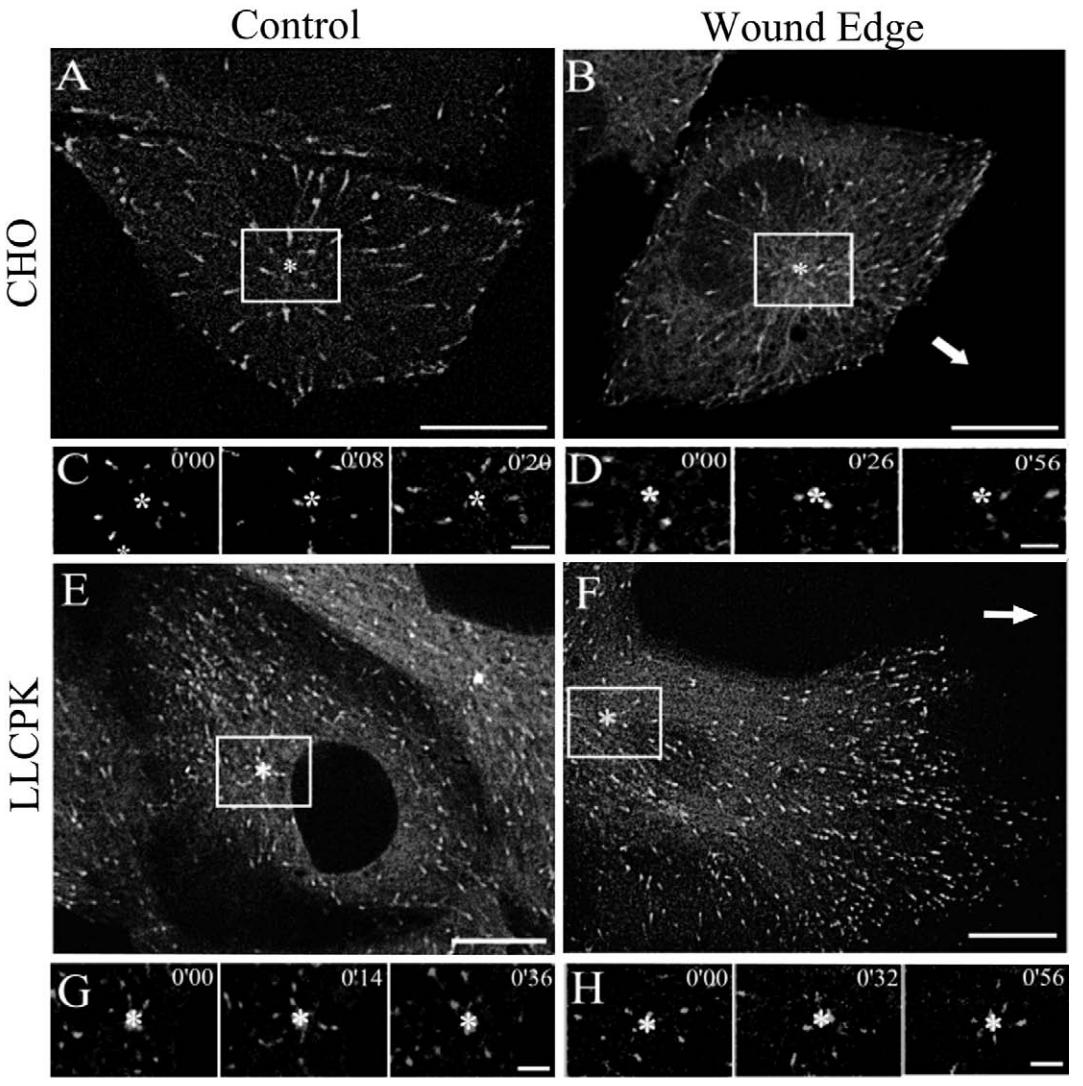

Fig. 2. Microtubule nucleation at the centrosome is not biased towards the wound edge. Confocal images show non-wound-edge controls (A,E) and wound-edge cells (B,F). (A-D) CHO fibroblasts and (E-H) LLCPK1 epithelial cells expressing EB1-GFP to mark the plus ends of growing microtubules; not all cells in the culture express the construct, and these cells cannot be detected in the fluorescence micrographs. The asterisk (*) marks the position from which the growing plus ends originate. Arrows indicate direction of migration into the wound. The boxed region from individual frames of the corresponding movie sequences are shown in C, D, G and H. Movies of the cells shown are in supplementary material Movies 1 and 2. Time is indicated in minutes and seconds in the upper right corner. Scale bars: 20 μm (A,B), 10 μm (E F) and 5 μm (C,D,G,H).

Table 1. Microtubule nucleation at the centrosome

Cell line	Centrosome no.	Control (*n*)	Wound edge (*n*)
CHO	1	14.4±1.7 (8)	8.7±3.1* (12)
	2	23.1±3.7 (9)	15.4±4.5* (12)
LLCPK1	1	14.1±5.8 (8)	13.9±1.5 (8)
	2	22.4±5.8 (10)	18.5±2.3 (10)

*Significantly different from controls at 95% confidence level.
n=number of cells.

CHO cells (Fig. 2B; see Movie 2 in supplementary material), however, the rate of nucleation was statistically significantly reduced when compared with non-wound-edge cells (8.7±3.1 in wound edge vs 14.4±1.7 in controls; Table 1). A similar reduction was observed for cells in G2 (15.4±4.5 in wound-edge vs 23.1±3.7 in controls; Table 1). The decrease in nucleation events observed in wound-edge CHOs may result from a decrease in the tubulin dimer level resulting from the generation of stable microtubules (see Discussion).

Our nucleation data for cells containing one or two centrosomes does not reveal a precise two-fold increase in total nucleations when two centrosomes are present (Table 1). This situation could have resulted from problems in the visual detection of nucleation events that occurred between the duplicated centrosomes. However, when G2 cells with separated and non-separated centrosomes were analyzed separately, there was no difference between the two groups (data not shown). Alternatively, daughter centrioles may nucleate fewer microtubules than mother centrioles resulting in less than twice the number of nucleations in G2 cells (Andersen, 1999).

In addition to examining the rate of nucleation at the centrosome, we questioned whether or not growth events were uniformly distributed around the centrosome or if there is a directional bias in nucleation relative to the wound edge (see Materials and Methods). In both fibroblasts and epithelial cells, we did not detect any directional bias in growth events at the centrosome for cells with either one or two centrosomes (Fig. 2; Table 2).

Microtubule growth at the cell periphery

We wanted to determine if growing microtubules were uniformly distributed in the cell periphery. We measured the number of EB1-GFP dashes in a 7 μm wide region along the leading and trailing edges and then calculated the number of leading and trailing edge growth events per unit area (μm^2). The average number of growth events/μm^2 was not different in leading and trailing edges (Fig. 3, Table 3). However, we noticed that growing microtubules were not uniformly distributed along the leading edge of EB1-GFP LLCPK1 cells. We compared the number of growth events in the central region of the leading edge and at the edge, where the cell contacts its neighbors. The results show that the number of growing plus-ends at the edge (see Movie 3 in supplementary material) was approx. twofold greater than the number in the center; this difference was statistically significant. By contrast, growth events were uniformly distributed across the trailing edge of LLCPK1 cells and across both the leading and trailing edges of CHO fibroblasts (not shown). Interestingly, although we observed a greater rate of microtubule nucleation in G2 cells,

Table 2. Microtubule nucleation toward and away from the wound edge

Cell line	Centrosome no.	Leading nuc/min* (*n*)	Trailing nuc/min* (*n*)	L:T ratio†
CHO	1	3.9±1.2 (12)	4.8±2.1 (12)	0.9±0.4
	2	7.2±2.2 (12)	7.3±2.9 (12)	1.1±0.3
LLCPK1	1	6.6±0.7 (8)	7.3±1.1 (8)	0.9±0.1
	2	9.3±1.9 (10)	9.2±0.7 (10)	1.0±0.2

*Nucleations/minute.
†Leading nucleations/trailing nucleations.
n=number of cells.

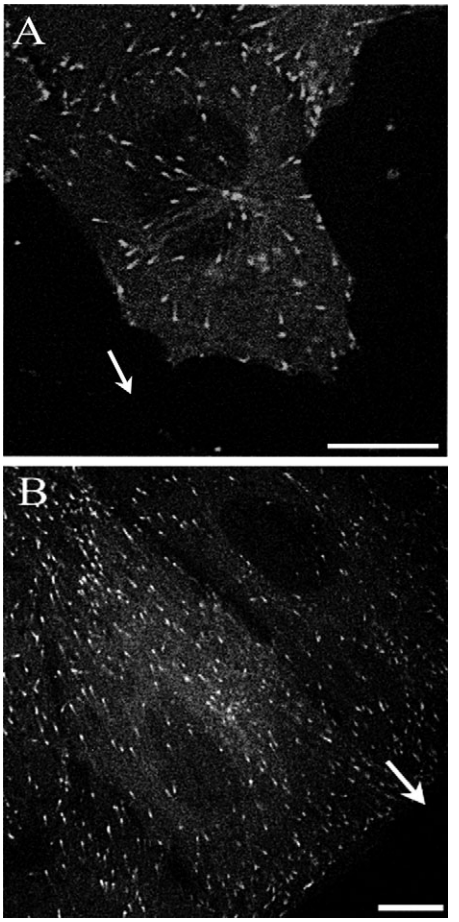

Fig. 3. Microtubule growth events are uniform at the cell periphery. Confocal micrographs of a CHO fibroblast (A) and an LLCPK1 epithelial cell (B) expressing EB1-GFP. The average number of growth events per unit area is not statistically different at the leading and trailing edges of either CHO or LLCPK1 cells. Scale bars: 5 μm.

Table 3. Microtubule growth at the cell periphery

Cell line	Leading edge (GFP-EB1 dashes/100 μm^2)	Trailing edge (GFP-EB1 dashes/100 μm^2)
CHO	16.1±1.3 (*n*=7 cells)	14.0±1.4 (*n*=6 cells)
LLCPK1	15.0±3.5 (*n*=6 cells)	18.3±3.6 (*n*=7 cells)

Table 4. Microtubule growth rates

Cell line	Position	Growth rate* (μm/min)
CHO	Leading edge	16.0±6.8 (*n*=299)
	Trailing edge	17.2±7.7 (*n*=335)
LLCPK1	Leading edge	17.9±7.7 (*n*=323)
	Trailing edge	19.0±8.8 (*n*=300)

*Instantaneous rates measured from positions of GFP-EB1 dashes in sequential frames of a time-lapse series.
n=number of measurements.

growing microtubules/μm^2 were similar in the periphery of G1 and G2 cells (see Discussion).

Microtubule growth rates

In addition to quantifying the rate of nucleation, we determined microtubule growth rates in the leading and trailing edges of wound-edge cells by tracking individual EB1-GFP dashes as they emerged from the centrosome and grew outwards (Table 4). In both CHO fibroblasts and LLCPK1 epithelial cells, the instantaneous rate of microtubule growth was similar for microtubules extending toward the front and rear of the cell (Table 4). In CHO cells, the average microtubule growth rates in the leading and trailing edges were 16.0±6.8 and 17.2±7.7 μm/minute, respectively. In LLCPK1 cells the average growth rates were 17.9±7.7 μm/minute in the leading edge and 19.0±8.8 μm/minute the trailing edge (Table 4). These differences are not statistically significant.

Previous work with fibroblasts has shown that a subset of microtubules is characterized by very rapid rates of growth (35-60 μm/minute). It has been suggested that these microtubules are released from the centrosome and transported as they elongate at the plus-end, thus accounting for the apparent rapid growth rate. Analysis of the distribution of instantaneous rates for LLCPK1-EB1-GFP cells and CHO cells expressing EB1-GFP showed that less than 10% of the rates were >30 μm/minute (data not shown) and these rates were interspersed with slower instantaneous rates of growth. Thus our data do not provide evidence for a subpopulation of microtubules with a sustained faster growth rate (Abal et al., 2002).

Many of the plus-ends grew persistently from the centrosome, reaching to the cell edge before the comet of EB1-GFP was lost (Komarova et al., 2002). In some cases, growing plus-ends were observed to reach the edge of the cell and continue to grow along the edge before the comet was lost. This observation suggests that the cell edge does not always alter the behavior of the microtubule end, and at least in some cases, the plus-end can change its trajectory and continue to grow.

Microtubule dynamic instability is asymmetric in polarized, wound-edge cells

Our results demonstrate that growing microtubule plus-ends are distributed in a relatively uniform manner in wound-edge cells (Figs 2, 3), but that the microtubule cytoskeleton is polarized, with more microtubules extending toward the wound edge (Fig. 1). To understand how this asymmetry is generated, we measured the parameters of microtubule dynamic instability in leading and trailing edges of living wound-edge

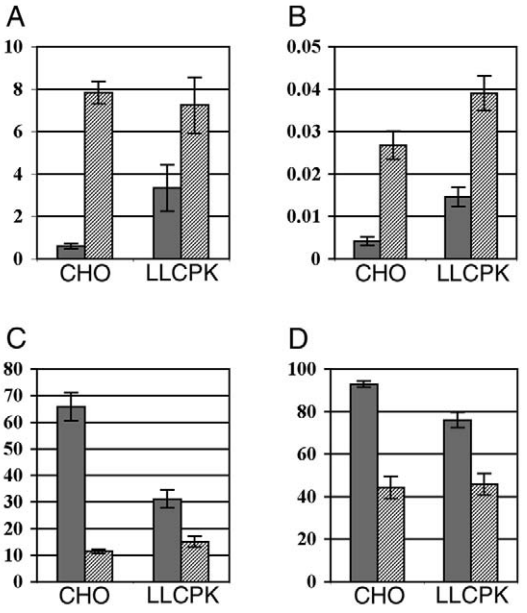

Fig. 4. Microtubule dynamic instability differs in leading and trailing edges of CHO and LLCPK1 cells. Solid bars, leading edges; hatched bars, trailing edges. (A) Dynamicity, (B), catastrophe frequency, (C) pause duration, (D) Percentage time in pause. Microtubules in trailing edges have more catastrophes and greater overall dynamicity (A,B); microtubules in leading edges spend more time in pause and have longer pause durations (C,D). Error bars show standard error of the mean.

fibroblasts and epithelial cells expressing GFP-tubulin (Fig. 1C,D). In both cell lines, microtubules extending away from the wound edge were more dynamic than those extending toward the wound (Fig. 4, Table 5). The frequency of catastrophe, the transition from growth to shortening, was lower in leading edges, as compared with trailing edges, of both cell lines (Fig. 4); rescue transitions were similar in leading and trailing edges (Table 5). The average duration of pause events was also greater in leading edges, as was the percentage of time spent in pause (Fig. 4). The increase in the percentage of time spent in pause was accompanied by decreases in the percentage of time spent in growth and shortening. Most microtubules in leading edges showed periods of pause interspersed with more dynamic activity, indicating that microtubules at the leading edge are not permanently stabilized, but show reduced dynamic activity. Finally, dynamicity, the sum of the growth and shortening distances per unit time, was greater in trailing compared to leading edges (Fig. 4). Overall, the values for dynamic parameters in the trailing edges are remarkably similar for both cell lines, with greater variation in leading edges (Table 5).

Rho regulates microtubule dynamics in trailing but not leading edges

Previous work has shown that Rho and its downstream effector mDia are required to generate detyrosinated, Glu-microtubules, facing the wound edge (Cook et al., 1998; Palazzo et al., 2001). However, Glu-microtubules represent only a subset of microtubules and cannot be assayed in living

Table 5. Microtubule dynamic behavior in leading and trailing edges of the wound edge cells

	CHO cells		LLCPK cells	
Dynamic parameters	Leading edge (42 MTs)	Trailing edge (41 MTs)	Leading edge (33 MTs)	Trailing edge (30 MTs)
Growth				
Rate	11.04±6.32	11.63±5.97	8.93±6.24	9.08±6.63
Distance	1.10±0.60	1.84±1.73	1.07±0.55	1.36±1.07
Duration	7.05±4.30	10.21±9.19	9.16±5.83	10.12±6.64
% Time growth	3.6±6.7†	38.0±18.3	14.7±14.9†	31.6±17.2
Shrink				
Rate	14.02±9.55	17.04±7.79	11.90±7.85†	16.39±7.48
Distance	0.95±0.38†	2.67±2.94	1.21±0.78†	2.03±1.85
Duration	5.65±4.34	8.74±7.64	6.54±2.45	7.66±5.38
% Time shrink	2.5±5.6†	19.6±13.1	9.2±8.0†	22.6±13.9
Pause				
Duration	62.78±43.8†	9.87±10.90	31.17±32.9†	15.10±20.09
% Time Pause	93.9±8.4†	42.4±16.2	76.1±20.5†	45.9±27.4
Rescue frequency (s^{-1})	0.246±0.171	0.131±0.119	0.163±0.089	0.134±0.108
Catastrophe frequency (s^{-1})	0.005±0.008†	0.030±0.022	0.015±0.01†	0.039±0.022
Dynamicity (μm/min)	0.60±0.76†	7.88±3.32	3.35±6.27*	7.24±7.22

*Significant from trailing edge cells at 95% confidence level.
†Significant from trailing edge cells at 99% confidence level.
All statistics analyzed using a Student's *t*-test.

cells. To determine the role of Rho in regulating microtubule behavior in leading and trailing edges of living cells, LLCPK1α cells were injected with C3 transferase, an inhibitor of Rho activity (Nobes and Hall, 1999; O'Connell et al., 1999; Sekine et al., 1989). Injection of C3 resulted in a disruption of F-actin stress fibers, demonstrating that the C3 was active (data not shown). Surprisingly, microtubule dynamics in the leading edges of C3-injected cells were not statistically significantly altered by inhibition of Rho activity. However, several parameters of microtubule dynamics in trailing edges were significantly changed (Fig. 5). The rates (Fig. 5A,B), distances (Fig. 5C,D) and duration (not shown) of both growth and shortening events were all statistically significantly greater in the trailing edges of C3-injected cells; overall dynamicity was also statistically significantly increased in trailing edges of C3-injected cells from 6.4 to 9.3 μm/minute. The frequencies of catastrophe and rescue and pause duration (Fig. 5F) were not statistically significantly changed following C3 injection.

Discussion

Microtubule nucleation and growth in wound-edge cells

To understand how an asymmetric microtubule array is generated in polarized wound-edge cells, we measured microtubule growth in the periphery and nucleation events at the centrosome using EB1-GFP to mark microtubule plus-ends and microtubule dynamic instability parameters in the leading and trailing lamella of wound-edge cells, using GFP-tubulin to label microtubules. Our results demonstrate that nucleation from the centrosome is not directionally biased, and therefore an asymmetric microtubule array does not result from asymmetric nucleation. Following nucleation, similar numbers of growing microtubule plus-ends were observed in leading and trailing edges, demonstrating that persistent microtubule growth is also symmetric in polarized cells. Although the number of growing microtubules/unit area averaged across the leading and trailing edges was similar, a greater number of

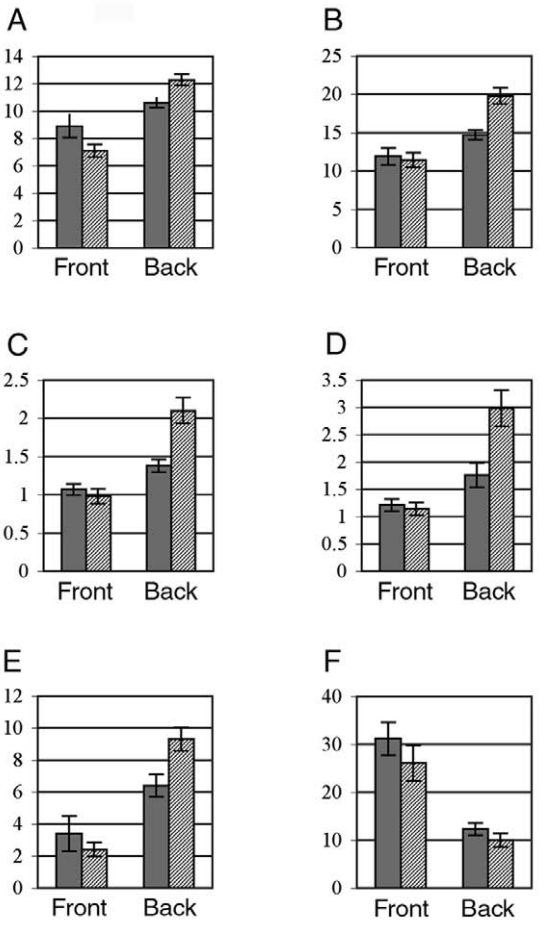

Fig. 5. RhoA regulates microtubule dynamics in trailing edges. Solid bars, control cells, hatched bars, C3-injected cells; Front, leading edges; Back, trailing edges. (A) growth rate, (B) shortening rate, (C) growth distance, (D) shortening distance, (E) dynamicity and (F) pause duration.

growing microtubules/unit area was detected at the edges of epithelial cells that contacted neighboring cells. Because microtubule growth has been shown to respond to tension (Kaverina et al., 2002), the data suggest that these areas are sites where tension is applied to the cells, thus locally promoting microtubule growth. Our results also demonstrate that the number of growing microtubules/unit area is constant as cells progress from G1 to G2, demonstrating that the increased microtubule nucleation resulting from centrosome duplication is compensated for by the increase in cell size (Piehl and Cassimeris, 2003). We conclude that microtubule nucleation provides a relatively uniform source of growing microtubule plus-ends throughout the cytoplasm of mammalian cells.

The regulation of microtubule nucleation at the centrosome is not yet well understood. Nucleation increases dramatically as cells enter mitosis, with a maximal increase in anaphase of sevenfold over interphase values (Piehl and Cassimeris, 2003). Increased recruitment of γ-tubulin to the centrosome can account for some, but not all, of the increase in nucleation (Piehl et al., 2004). Microtubule nucleation from the centrosome in control, non-wound-edge cells, was not cell-type-specific, in contrast to microtubule dynamic instability in the periphery, which is cell-type-specific (Komarova et al., 2002; Shelden and Wadsworth, 1993). These data indicate that events at the periphery, not at the centrosome, are likely to be responsible for the cell-type-specific features of microtubule dynamic turnover. In CHO fibroblasts at the wound edge, however, the number of nucleation events was significantly reduced as compared to control, non-wound-edge cells. One possible explanation for this observation is that the observed accumulation of microtubules in the leading edge of CHO fibroblasts reduces the tubulin dimer concentration and thus lowers the rate of nucleation. Consistent with this possibility is the observation that nucleation was not reduced in wound-edge LLCPK1 cells and these cells do not accumulate microtubules in the leading edge to the extent observed in CHO cells. Cells expressing EB1-GFP will provide a useful tool to study the regulation of microtubule nucleation and growth in living cells (Piehl and Cassimeris, 2003; Rogers et al., 2002; Tirnauer and Bierer, 2000).

Microtubule dynamic instability is asymmetric in wound-edge cells

We measured striking differences in microtubule dynamic instability behavior in leading and trailing edges of living, wound-edge cells. These differences were similar to those observed previously in protrusive and non-protrusive regions of growth factor-treated migrating cells (Wadsworth, 1999). The differential microtubule behavior that we measured is accomplished by relatively subtle changes in dynamic instability that suppress, but do not abolish, the dynamic behavior of lamellar microtubules.

We found that inhibition of RhoA with C3 transferase resulted in increased microtubule dynamic behavior in the trailing edge, demonstrating that RhoA activity contributes to microtubule stability in this region. In the trailing edges of C3-treated cells, the transition frequencies were not altered, but the rates and durations of growth and shortening were increased. This mechanism of action is distinct from that measured as cells traverse the cell cycle (Belmont et al., 1990; Rusan et al., 2001), where changes in the transition frequencies are typically observed.

Surprisingly, treatment with C3 transferase did not significantly alter microtubule dynamics in the leading edge. Previous studies have shown that RhoA activity is required for the formation of post-translationally modified Glu-microtubules in cultured cells (Cook et al., 1998); post-translational modifications are correlated with microtubule stability (Khawaja et al., 1988). One explanation for this discrepancy is that the generation of stable microtubules in the leading edge requires RhoA (Cook et al., 1998), but maintenance of this microtubule subpopulation does not. This is consistent with the observation that an asymmetric microtubule array was maintained following expression of RhoN19. An alternative explanation is that the subset of microtubules identified by the anti-Glu antibodies does not correspond to the microtubules we measured near the margin of live cells. This explanation is consistent with the observation that many Glu-positive microtubules are located in the perinuclear region and that Glu microtubules represent only a relatively small fraction of microtubules in the lamella. Our data also indicates that Rho-independent pathways can contribute to microtubule stability, especially in the leading edge. Previous work has identified the CLASP proteins that localize to the distal plus-ends of microtubules in the leading, but not trailing edge (Akhmanova et al., 2001). These proteins, which are regulated by PI 3-kinase and GSK-3β, may contribute to RhoA-independent microtubule stability in the leading edge (Akhmanova et al., 2001).

Contribution of differential microtubule dynamic turnover to cell polarity and migration

The differential behavior of microtubules in the front and rear of polarized cells is likely to contribute to directed motility (Kaverina et al., 1999; Kaverina et al., 1998). Historically, the observation that post-translationally modified microtubules are oriented toward the direction of migration led to the idea that microtubule stability is important for directed migration (Gundersen and Bulinski, 1988). In support of this view, a dominant-negative EB1 construct that prevents microtubule stabilization has been shown to inhibit cell migration (Wen et al., 2004). However, treatment of cells with low doses of microtubule poisons that suppress microtubule dynamics, also inhibits directed migration, reinforcing the idea that dynamic microtubules are necessary for migration (Liao et al., 1995). We favor the possibility that both dynamic and stable microtubules contribute to directed migration, and the balance between these populations is important for cell migration. Local activation of regulators of microtubule dynamics could result in different steady state polymer levels in the two locations and distinct parameters of dynamic instability. The continual generation of new microtubules at the centrosome may ensure that the microtubule population can readily respond to changing external stimuli (Akhmanova et al., 2001; Etienne-Manneville and Hall, 2001; Ridley et al., 2003; Rodriguez et al., 2003).

How might stable and dynamic microtubules contribute to cell migration? During cell migration, adhesions in the rear must be released and new adhesions established in the front

(Ridley et al., 2003). Microtubules target sites of adhesion and more frequent targeting correlates with more rapid turnover of the adhesion (Kaverina et al., 1999; Kaverina et al., 1998; Rodriguez et al., 2003). Our observations support the possibility that increased microtubule dynamics in the trailing edge could locally increase targeting events and thus regulate the lifetime of an adhesion, thereby contributing to migration.

In summary, our results demonstrate that microtubule nucleation events are uniformly distributed around the centrosome in wound-edge cells and that the number of growing microtubule plus-ends is similar in the periphery of leading and trailing edges. In marked contrast to nucleation, microtubule dynamic instability is asymmetric in wound-edge cells: microtubules in the trailing edge are more dynamic than those facing the leading edge. Microtubule dynamics in the leading edge were insensitive to inhibition of RhoA with C3 transferase, whereas microtubule dynamics in the trailing edge were increased under these conditions. Our data demonstrate that factors in addition to Rho contribute to microtubule behavior in the leading edge of wound-edge cells.

We thank Allan Hall for providing the RhoA and Cdc42 constructs used in these experiments; Anne Ridley for advice concerning nuclear microinjection; Alenka Lovey-Wheeler and Dale Callaham for assistance with confocal microscopy. Special thanks to Corey Godfrey for assistance with microtubule tracking, Nasser M. Rusan for help preparing the figures. This work was supported by NIH grant GM059057 awarded to P. Wadsworth.

References

Abal, M., Piel, M., Bouckson-Castaing, V., Mogensen, M. M., Sibarita, J.-B. and Bornens, M. (2002). Microtubule release from the centrosome in migrating cells. *J. Cell Biol.* **159**, 731-737.

Akhmanova, A., Hoogenraad, C. C., Drabek, K., Stepanova, T., Dortland, B., Verkerk, T., Vermeulen, W., Burgering, B. M., De Zeeuw, C. I., Grosveld, F. et al. (2001). CLASPS are CLIP-115 and -170 Associating proteins involved in the regional regulatin of microtubule dynamics in motile fibroblasts. *Cell* **104**, 923-935.

Alberts, B., Johnson, A., Lewis, J., Raff, M., Roberts, K. and Walter, P. (2002). *Molecular Biology of the Cell*. 3rd edn: Garland Publishing, Inc., New York and London.

Andersen, S. S. L. (1999). Molecular characteristics of the centrosome. *Int. Rev. Cytol.* **187**, 51-109.

Belmont, L. D., Hyman, A. A., Sawin, K. E. and Mitchison, T. J. (1990). Real-time visualization of cell cycle dependent changes in microtubule dynamics in cytoplasmic extracts. *Cell* **62**, 579-589.

Buck, K. B. and Zheng, J. Q. (2002). Growth cone turning induced by direct local modification of microtubule dynamics. *J. Neurosci.* **22**, 9358-9367.

Cassimeris, L. (1993). Regulation of MT dynamic instability in living cells. *Cell Motil. Cytoskeleton* **26**, 275-281.

Cook, T. A., Nagasaki, T. and Gundersen, G. G. (1998). Rho guanosine triphosphatase mediates the selective stabilization of microtubules induced by lysophosphatidic acid. *J. Cell Biol.* **141**, 175-185.

Etienne-Manneville, S. and Hall, A. (2001). Integrin-mediated activation of Cdc42 controls cell polarity in migrating astrocytes through PKC. *Cell* **106**, 489-498.

Gundersen, G. G. and Bulinski, J. C. (1988). Selective stabilization of microtubules oriented toward the direction of cell migration. *Proc. Natl. Acad. Sci. USA* **85**, 5946-5950.

Hall, A. (1998). Rho GTPases and the actin cytoskelton. *Science* **279**, 509-519.

Kao, F.-T. and Puck, T. T. (1968). Genetics of somatic mammalian cells, VII. Induction and isolation of nutritional mutants in Chinese hamster cells. *Proc. Natl. Acad. Sci. USA* **60**, 1275-1280.

Kaverina, I., Rottner, K. and Small, J. V. (1998). Targeting, capture, and stabilization of microtubules at focal adhesions. *J. Cell Biol.* **142**, 181-190.

Kaverina, I., Krylyshkina, O. and Small, J. V. (1999). Microtubule targeting of substrate contacts promotes their relaxation and dissociation. *J. Cell Biol.* **146**, 1033-1044.

Kaverina, I., Krylyshkina, O., Beningo, K. A., Anderson, K., Wang, Y.-L. and Small, J. V. (2002). Tensile stress stimulates microtubule outgrowth in living cells. *J. Cell Sci.* **115**, 2283-2291.

Khawaja, S., Gundersen, G. G. and Bulinski, J. C. (1988). Enhanced stability of microtubules enriched in detyrosinated tubulin is not a direct function of detyrosination level. *J. Cell Biol.* **106**, 141-149.

Kirschner, M. W. and Mitchinson, T. (1986). Beyond self assembly; From microtubule to morphogenesis. *Cell* **45**, 329-342.

Komarova, Y. A., Vorobjev, I. and Borisy, G. G. (2002). Life cycle of microtubules: persistent growth in the cell interior, asymmetric transition frequencies and effects of the cell boundry. *J. Cell Sci.* **115**, 3527-3539.

Liao, G., Nagasaki, T. and Gundersen, G. G. (1995). Low concentrations of nocodazole interfere with fibroblast locomotion without significantly affecting microtubule level: implications for the role of dynamic microtubules in cell locomotion. *J. Cell Sci.* **108**, 3473-3483.

Mitchison, T. J. and Kirschner, M. W. (1984). Dynamic instability of microtubule growth. *Nature* **312**, 237-242.

Murthy, K. and Wadsworth, P. (2005). Myosin-II-dependent localization and dynamics of F-actin during cytokinesis. *Curr. Biol.* **15**, 724-731.

Nobes, C. D. and Hall, A. (1999). Rho GTPases control polarity, protrusion and adhesion during cell movement. *J. Cell Biol.* **144**, 1235-1244.

O'Connell, C. B., Wheatley, S. P., Ahmed, S. and Wang, Y.-L. (1999). The small GFP-binding protein Rho regulates cortical activities in cultured cells during division. *J. Cell Biol.* **144**, 305-313.

Palazzo, A., Cook, T. A., Alberts, A. S. and Gundersen, G. G. (2001). mDia mediates Rho-regulated formation and orientation of stable microtubules. *Nat. Cell Biol.* **3**, 723-730.

Piehl, M. and Cassimeris, L. (2003). Organization and dynamics of growing microtubule plus ends during early mitosis. *Mol. Biol. Cell* **14**, 916-925.

Piehl, M., Tulu, U. S., Wadsworth, P. and Cassimeris, L. (2004). Centrosome maturation: measurement of microtubule nucleation throughout the cell cycle using GFP tagged EB1. *Proc. Natl. Acad. Sci. USA* **101**, 1584-1588.

Ridley, A. J. and Hall, A. (1992). The small GTP-Binding protein rho regulates the assembly of focal adhesions and actin stress fibers in response to growth factors. *Cell* **70**, 389-399.

Ridley, A. J., Schwartz, M. A., Burridge, K., Firtel, R. A., Ginsberg, M. H., Borisy, G. G., Parsons, J. T. and Horwitz, A. R. (2003). Cell migration: integrating signals from front to back. *Science* **302**, 1704-1709.

Rodionov, V., Nadezhdina, E. and Borisy, G. (1999). Centrosomal control of microtubule dynamics. *Proc. Natl. Acad. Sci. USA* **96**, 115-120.

Rodriguez, O. C., Schaefer, A. W., Mandato, C. A., Forscher, P., Bement, W. M. and Waterman-Storer, C. M. (2003). Conserved microtubule-actin interactions in cell movement and morphogenesis. *Nat. Cell Biol.* **5**, 599-609.

Rogers, S. L., Rogers, G. C., Sharp, D. J. and Vale, R. D. (2002). Drosophila EB1 is important for proper assembly, dynamics and positioning of the mitotic spindle. *J. Cell Biol.* **158**, 873-884.

Rose, G. G., Pomerat, C. M., Shindler, T. O. and Trunnel, J. B. (1958). A cellophane strip technique for culturing tissue in multipurpose culture chambers. *J. Biophys. Biochem. Cytol.* **4**, 761-764.

Rusan, N. M. and Wadsworth, P. (2005). Centrosome fragments and microtubules are released and transported asymetrically away from division plane in anaphase. *J. Cell Biol.* **168**, 21-28.

Rusan, N. M., Fagerstrom, C., Yvon, A. C. and Wadsworth, P. (2001). Cell cycle dependent changes in microtubule dynamics in living cells expressing GFP-alpha tubulin. *Mol. Biol. Cell* **12**, 971-980.

Sammak, P. J. and Borisy, G. G. (1988). Direct observation of microtubule dynamics in living cells. *Nature* **332**, 724-726.

Schulze, E. and Kirschner, M. (1988). New features of microtubule behavior observed in vivo. *Nature* **334**, 356-359.

Sekine, A., Fujiwara, M. and Narumiya, S. (1989). Asparagine residue in the rho gene product is the modification site for botulinum ADP-ribosyltransferase. *J. Biol. Chem.* **91**, 8602-8605.

Shelden, E. and Wadsworth, P. (1993). Observation and quantification of individual microtubule behavior in vivo: Microtubule dynamics are cell-type specific. *J. Cell Biol.* **120**, 935-945.

Suter, D. M. and Forscher, P. (1998). An emerging link between cytoskeletal dynamics and cell adhesion molecules in growth cone guidance. *Curr. Opin. Neurosci.* **8**, 106-116.

Tanaka, E. and Kirschner, M. (1991). Microtubule behavior in the growth

cones of living neurons during axon elongation. *J. Cell Biol.* **115**, 345-363.

Tirnauer, J. S. and Bierer, B. E. (2000). EB1 proteins regulate microtubule dynamics, cell polarity, and chromosome stability. *J. Cell Biol.* **149**, 761-766.

Vasiliev, J. M. (1991). Polarization of pseudopodial activities: cytoskeletal mechanisms. *J. Cell Sci.* **98**, 1-4.

Wadsworth, P. (1999). Regional regulation of microtubule dynamics in polarized, motile cells. *Cell Motil. Cytoskeleton* **42**, 48-59.

Waterman-Storer, C. M. and Salmon, E. D. (1997). Actomyosin-based retrograde flow of microtubules in the lamella of migrating epithelial cells influences microtubule dynamic instability, induces microtubule breakage and generates non-centrosomal microtubules. *J. Cell Biol.* **139**, 417-434.

Waterman-Storer, C. M., Salmon, W. C. and Salmon, E. D. (2000). Feedback interactions between cell-cell adherens junctions and cytoskeletal dynamics in newt lung epithelial cells. *Mol. Biol. Cell* **11**, 2471-2483.

Wen, Y., Eng, C. H., Schmoranzer, J., Cabrera-Poch, N., Morris, E. J. S., Chen, M., Wallar, B. J., Alberts, A. S. and Gundersen, G. G. (2004). EB1 and APC bind to mDia to stabilize microtubules downstream of Rho and promote cell migration. *Nat. Cell Biol.* **6**, 820-830.

Yvon, A. C. and Wadsworth, P. (1997). Non-centrosomal microtubule formation and measurement of minus end microtubule dynamics in A498 cells. *J. Cell Sci.* **110**, 2391-2401.

Yvon, A. C., Walker, J. W., Danowski, B. A., Fagerstrom, C., Khojakov, A. and Wadsworth, P. (2002). Centrosome reorientation in wound edge cells is cell type specific. *Mol. Biol. Cell* **13**, 1871-1880.